International Journal of Digital Earth

ISSN: 1753-8947 (Print) 1753-8955 (Online) Journal homepage: https://www.tandfonline.com/loi/tjde20

Global characterization and monitoring of forest cover using Landsat data: opportunities and challenges

John R. Townshend , Jeffrey G. Masek , Chengquan Huang , Eric F. Vermote , Feng Gao , Saurabh Channan , Joseph O. Sexton , Min Feng , Raghuram Narasimhan , Dohyung Kim , Kuan Song , Danxia Song , Xiao-Peng Song , Praveen Noojipady , Bin Tan , Matthew C. Hansen , Mengxue Li & Robert E. Wolfe

To cite this article: John R. Townshend , Jeffrey G. Masek , Chengquan Huang , Eric F. Vermote , Feng Gao , Saurabh Channan , Joseph O. Sexton , Min Feng , Raghuram Narasimhan , Dohyung Kim , Kuan Song , Danxia Song , Xiao-Peng Song , Praveen Noojipady , Bin Tan , Matthew C. Hansen , Mengxue Li & Robert E. Wolfe (2012) Global characterization and monitoring of forest cover using Landsat data: opportunities and challenges, International Journal of Digital Earth, 5:5, 373-397, DOI: 10.1080/17538947.2012.713190

To link to this article: https://doi.org/10.1080/17538947.2012.713190

Published online: 23 Aug 2012.

International Journal of Digital Earth,
Vol. 5, No. 5, September 2012, 373–397

Taylor & Francis
Taylor & Francis Group

Global characterization and monitoring of forest cover using Landsat data: opportunities and challenges

John R. Townshend[a]*†, Jeffrey G. Masek[b], Chengquan Huang[a], Eric. F. Vermote[c], Feng Gao[d], Saurabh Channan[a], Joseph O. Sexton[a], Min Feng[a], Raghuram Narasimhan[a], Dohyung Kim[a], Kuan Song[c], Danxia Song[a], Xiao-Peng Song[a], Praveen Noojipady[a], Bin Tan[b], Matthew C. Hansen[c], Mengxue Li[c] and Robert E. Wolfe[b]

[a]*Global Land Cover Facility, Department of Geographical Sciences, University of Maryland, College Park, MD, USA;* [b]*Goddard Space Flight Center, National Aeronautics and Space Administration, Greenbelt, MD, USA;* [c]*Department of Geographical Sciences, University of Maryland, College Park, MD, USA;* [d]*USDA-ARS Hydrology and Remote Sensing Laboratory, Beltsville, MD, USA*

(*Received 30 June 2012; final version received 14 July 2012*)

The compilation of global Landsat data-sets and the ever-lowering costs of computing now make it feasible to monitor the Earth's land cover at Landsat resolutions of 30 m. In this article, we describe the methods to create global products of forest cover and cover change at Landsat resolutions. Nevertheless, there are many challenges in ensuring the creation of high-quality products. And we propose various ways in which the challenges can be overcome. Among the challenges are the need for atmospheric correction, incorrect calibration coefficients in some of the data-sets, the different phenologies between compilations, the need for terrain correction, the lack of consistent reference data for training and accuracy assessment, and the need for highly automated characterization and change detection. We propose and evaluate the creation and use of surface reflectance products, improved selection of scenes to reduce phenological differences, terrain illumination correction, automated training selection, and the use of information extraction procedures robust to errors in training data along with several other issues. At several stages we use Moderate Resolution Spectroradiometer data and products to assist our analysis. A global working prototype product of forest cover and forest cover change is included.

Keywords: Landsat; land cover; forest cover change; global mapping; global monitoring

1. Introduction

Realizing the potential of digital earth is dependent on many issues. One of the more important is to have internally consistent data-sets to populate it. The availability of global data-sets from Landsat has the potential to significantly improve the characterization of the Earth's land surface. This article outlines some of the opportunities offered by these data-sets with reference to land cover and specifically

*Corresponding author. Email: jtownshe@umd.edu
†The contributions of the different authors can be found in Appendix 1.

ISSN 1753-8947 print/ISSN 1753-8955 online

http://dx.doi.org/10.1080/17538947.2012.713190
http://www.tandfonline.com

to forest cover. It also analyzes some of the challenges in using these data-sets and how they can be overcome.

Land cover change is one of the most important drivers of changes in the Earth System. Of all land cover changes, deforestation is one of the most significant because of the magnitude of the resultant transformations in biophysical and ecological properties. Forest cover change (FCC) is highly relevant to the global carbon cycle, changes in the hydrological cycle, an understanding of the causes of changes in biodiversity and in understanding the rates and causes of land use change (Band 1993, Lal 1995, Houghton 1998, Pandey 2002). As a consequence, a number of national and international programs call for routine monitoring of global land cover FCCs, including the US Global Change Research Program (USGCRP 1999), Global Observation for Forest and Land Cover Dynamics (GOFC–GOLD) (Skole *et al*. 1998, Townshend *et al*. 2004), and the Global Climate Observing System (GCOS 2004).

In recent years there has been increasing emphasis on the need for products derived from Landsat resolution data. Requirements for such products are specified in many documents, including the Earth Science Data Record (ESDR) Community White Paper on Land Cover/Land Change (Masek *et al*. 2006) GOFC–GOLD's Fine Resolution design documents (Skole *et al*. 1998, Townshend *et al*. 2004) and the Integrated Global Observation Strategy's theme Integrated Global Observation of the Land theme (Townshend *et al*. 2010). Landsat-class resolutions are essential for land cover change detection because of the fine scale of many such changes especially those resulting from anthropogenic factors. A substantial proportion of the variability of land cover change has been shown to occur at resolutions below 250 m (Townshend and Justice 1988).

Estimating forest cover and measuring FCC are two of the more common uses of Landsat data. Landsat-class data have primarily been used at relatively local scales for forest change detection. Skole and Tucker (1993), Tucker and Townshend (2000), Steininger *et al*. (2001), Zhang *et al*. (2005), and Huang *et al.* (2007) are some of the few studies that executed wall-to-wall change detection at national scales. The Forest Resource Assessment of the United Nations' Food and Agriculture Organization (FAO) carried out limited Landsat-based sampling of change detection to assist the estimation of global tropical forest change rates between 1990 and 2000 (FAO 2001). DeFries *et al*. (2002) calculated global tropical forest change based on Advanced Very High Resolution Radiometer (AVHRR) data along with regional rates of changes estimated from Landsat data. Although the last two studies involved use of selected Landsat imagery and products, they were not used to carry out wall-to-wall change mapping for the entire study area. More recently Landsat samples combined with wall-to-wall data-sets have been used to provide estimates of forest loss in the tropics (Hansen *et al*. 2008) and subsequently for the globe (Hansen *et al*. 2010).

Previously, continental or even global-scale analysis using Landsat data was generally regarded as not feasible. This was because of the absence of well-registered multi-temporal data-sets, variations in sensors, the need for intensive human input during post-processing, variations in spectral responses of forests, the efforts needed to create data-sets for accuracy assessment, and the very large computational and storage demands in carrying out the analysis. Another major impediment was high data costs for global data-sets, a factor which was reduced after charging for Landsat data by the United States Geological Survey (USGS) was eliminated in 2008.

In this article, we discuss some of the challenges and strategies for the global use of Landsat data. In the present article 'global' refers to global wall-to-wall analysis of the Earth's land surface. We first discuss selection of data-sets and how some of the existing global data-sets published by the USGS should be refined. Then the need for surface reflectance products is discussed requiring atmospheric correction of the Landsat data-sets. Reduction of terrain effects through rectification is also essential as is correction for variations in solar illumination geometry. The challenges of assembling training data for global analysis are outlined as well as the requirement for data for error estimation. Procedures for global classification are discussed finally.

Computational power was once regarded as a major barrier to large area analysis of Landsat-class data. This is no longer the case as is demonstrated by the fact that the authors use a relatively modest set of Oracle 4150 servers, with 184 processing cores in total, which is capable of carrying out atmospheric correction of a complete Landsat global data-set in approximately 4 days and to carry out change detection using support vector machines (SVM) can be completed in approximately a week. Much more effort is normally required in the painstaking tasks of data-set assembly and performance assessment.

2. Selection of data-sets

The task of carrying out global analysis of Landsat data has been made immeasurably easier by the assembly of global data-sets by the USGS and NASA from existing archives. There are now several freely available Global Land Survey (GLS) data-sets (Table 1) (Gutman *et al*. 2008). These collections were created by identifying optimal scenes as close to the nominal date of the collection as available. For GLS 2005 out of the nearly 500,000 Landsat images that have been acquired around the globe during 2004–2007, the optimal 9500 scenes have been selected based on several criteria including acquisition date, cloud cover, gap-fill coverage, sensor choice, time of year and geographic uniformity (Gutman *et al*. 2008). As Table 1 shows some of the selected scenes had a somewhat different date of collection compared with the nominal one. Scenes were selected to minimize cloud cover and also to be closest to the date of maximum greenness (though see Section 4).

The use of GLS data-sets is facilitated by the fact that they have been standardized: all images are orthorectified in a Universal Transverse Mercator projection with a WGS84 datum, they have been resampled by cubic convolution, and are in a GeoTIFF data format. All epochs are registered to the GLS 2000 standard, which also forms the benchmark for the 'standard' L1T product from the US Landsat archive. Although the data are freely available from the USGS the large number of images in each data-set does pose logistical issues in downloading them.

Table 1. Global land survey collections.

Dataset	Acquisition year range	Number of Images
GLS 1975	1972–1987	7592
GLS 1990	1984–1997	7375
GLS 2000	1999–2003	8756
GLS 2005	2003–2008	10,273
GLS 2010	2007–2011	9000

Complete GLS data-sets on hard discs have been made available through the University of Maryland's Global Land Cover Facility (http://glcfapp.glcf.umd.edu:8080/order/index.jsp).

The way in which the images were selected has been progressively refined. Overall, the GLS 2005 data-set is superior to any other GLS in terms of data quality (Franks and Headley 2008). Previous GLS data-sets were single-sensor data-sets; Multispectral Scanner (MSS) was used for GLS 1975, Landsat 5 for GLS 1990, and Landsat 7 for GLS 2000. GLS 2005 had a richer selection of imagery to choose from by expanding the available data sources to include both Landsat 5 and 7, as well as images from Advanced Spaceborne Thermal Emission and Reflection Radiometer (ASTER) and Earth Observing Mission 1 (EO-1) (the use of the last was restricted to islands and reefs). Moreover, previous GLS data-sets put a high priority on cloud-free coverage, but at the expense of obtaining optimal leaf-on seasonality. Consequently, for some regions such as the dry deciduous tropics the GLS 1990 and GLS 2000 data-sets are less useful for mapping land cover conditions because many images were collected during leaf-off. In GLS 2005 greater weight is put on selecting leaf-on images at the expense of being as cloud-free as possible. The GLS 2010 data-set, covering imagery from 2009 to 2011 has just been released in early 2012.

Global Land Survey data-sets were preceded by NASA's global Landsat data-sets created by the Earthsat Corporation known as GeoCover for 1975, 1990, and 2000 (Tucker *et al*. 2004), and the Mid-Decadal GLS data-set jointly assembled by NASA and the USGS for 2005. Although GeoCover and GLS used essentially the same Landsat acquisitions for each location for the 1975, 1990, and 2000 epochs, there are differences: one key issue is that these earlier data-sets are at 28.5 m rather than the 30-m resolution of the GLS data-sets. Given the improvements in the processing and selection of images for the GLS global collections it is recommended that these are used in preference to the earlier ones.

3. Refinement of global data-sets

Comprehensive global coverage of Landsat data has become much more reliable, since the adoption of Landsat 7's Long-Term Acquisition Plan (Arvidson *et al*. 2001). This plan coupled with the astonishing longevity of Landsat 5 means there are essentially no gaps in Landsat records for GLS 2000, 2005, and 2010. Figure 1 shows the coverage for GLS 1975, 1990, 2000, and 2005. The initial GLS 1975 did have substantial gaps notably in South America, and no images were available for the entire eastern Siberia (Figure 1). Gaps in the former have been almost entirely filled using images from the Brazilian space agency INPE, which made scenes available from its archives. Unfortunately no substitute images have been found for northeast Asia.

Examination of the GLS data-sets revealed that some scenes had significant deficiencies relating in particular to inappropriate phenology of the selected images. This is especially troublesome for change detection since differences simply due to phenology may result in spurious identification of change. In theory the images that were chosen were close to peak greenness. A test was conducted for the Korean peninsula (Kim *et al*. 2011). For 2000 and 2005 most scenes were found to have images from very different times of years resulting in wildly improbable rates of

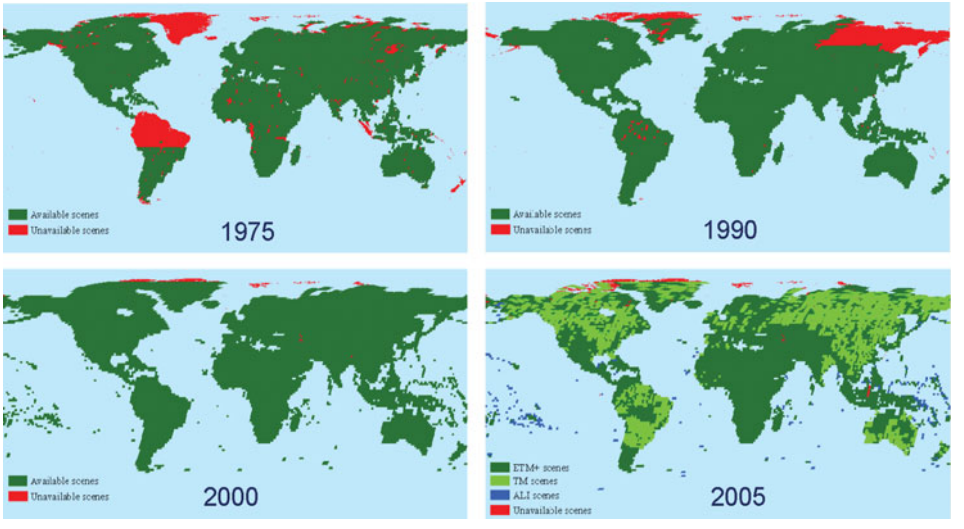

Figure 1. GLS data coverage. The large gap in coverage for South America for GLS 1975 has been filled by the data provided by INPE.

deforestation using spectral change detection methodology. A tool was constructed to allow automated querying of the USGS Global Visualization Viewer (GloVis) database (glovis.usgs.gov/). We used Moderate Resolution Spectroradiometer (MODIS) data to characterize the phenology of every scene and identify scenes acquired on dates within 75% of peak greenness. For 9 of the 11 scenes substitute images were found which had phenologies which met the above criterion. Figure 2 shows the resultant substitution for part of one scene and the greatly improved change results.

Subsequently we have performed a global analysis for GLS 2000 and 2005 and have identified many scenes where the selected images were collected at dates quite distant from the peak greenness. Figure 3 shows the substitutions for GLS 2000 and 2005. Our analysis somewhat exaggerated the severity of the problem since it includes scenes with a low phenological amplitude (e.g. tropical rain forests), where we do not need to substitute for such images.

It is unclear why the algorithm used for scene image selection for GLS failed at times to identify the best scenes. It may be that for some scenes additional images from non-US ground receiving stations may have been selected after initial selection from US holdings.

4. Production of surface reflectance images

In order to carry out a global analysis of Landsat data it is highly advantageous that the pixel values in all images represent the same physical values. The DNs in Landsat images do not directly represent any physical values and they vary depending on the Landsat mission and the agency generating the image. Coefficients are almost always provided with calibration coefficients so the DNs can be converted to top of the atmosphere radiance values. The latter however do not consistently represent surface conditions because of variable atmospheric effects and this in turn will hinder

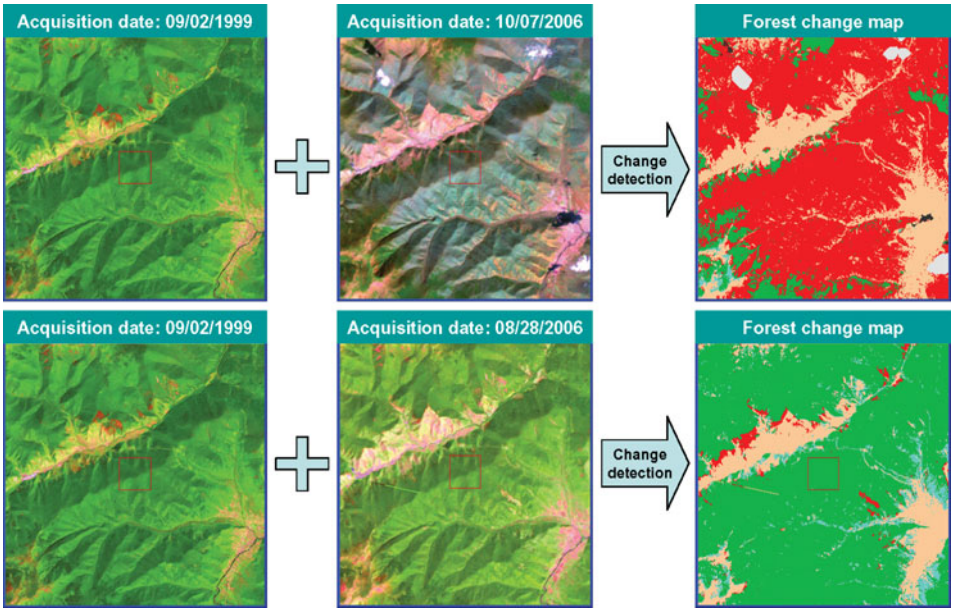

Figure 2. Spurious change detection caused by images with very different phenologies in deciduous woodland in South Korea (Kim *et al.* 2011) when using GLS data-set (top row). The substituted scene for 2006 clearly produces a much more realistic depiction of change than when the leaf off image is used (bottom row). The left and middle columns are the input Landsat images with bands 5, 4, 3 shown in red, green and blue. In the forest change maps (right column), persisting forest, persisting nonforest, forest loss and forest gain are in green, light pink, red and cyan, respectively.

automated global analysis. As a consequence it is highly desirable that we estimate surface reflectance by carrying out atmospheric correction so that we have more consistent imagery for mapping change. Also it helps in the development and use of cross-sensor algorithms using a common radiometric basis, for example, from MODIS and Landsat. In addition use of reflectances will allow us better to integrate observations with ground-based measurements of reflectance, and to facilitate use of canopy reflectance models to support, for example, the creation of biophysical products.

Before describing the methods used to generate the surface reflectance values through atmospheric correction, significant problems with the original GLS 1990 data-set's gain and bias coefficients need to be noted. Nearly half of these images were processed by different agencies using different versions of Landsat processing systems. As a result, different rescale gain and bias values were reported (Figure 4). These coefficients are not compatible with recent coefficients published by the USGS, that is, they yield incorrect top-of-atmosphere (TOA) reflectance values if used with the equations provided (Chander *et al.* 2004, 2009).

To obtain proper calibration coefficients these images need to be reprocessed from Level 0 using the current version of the USGS Landsat processing system. The

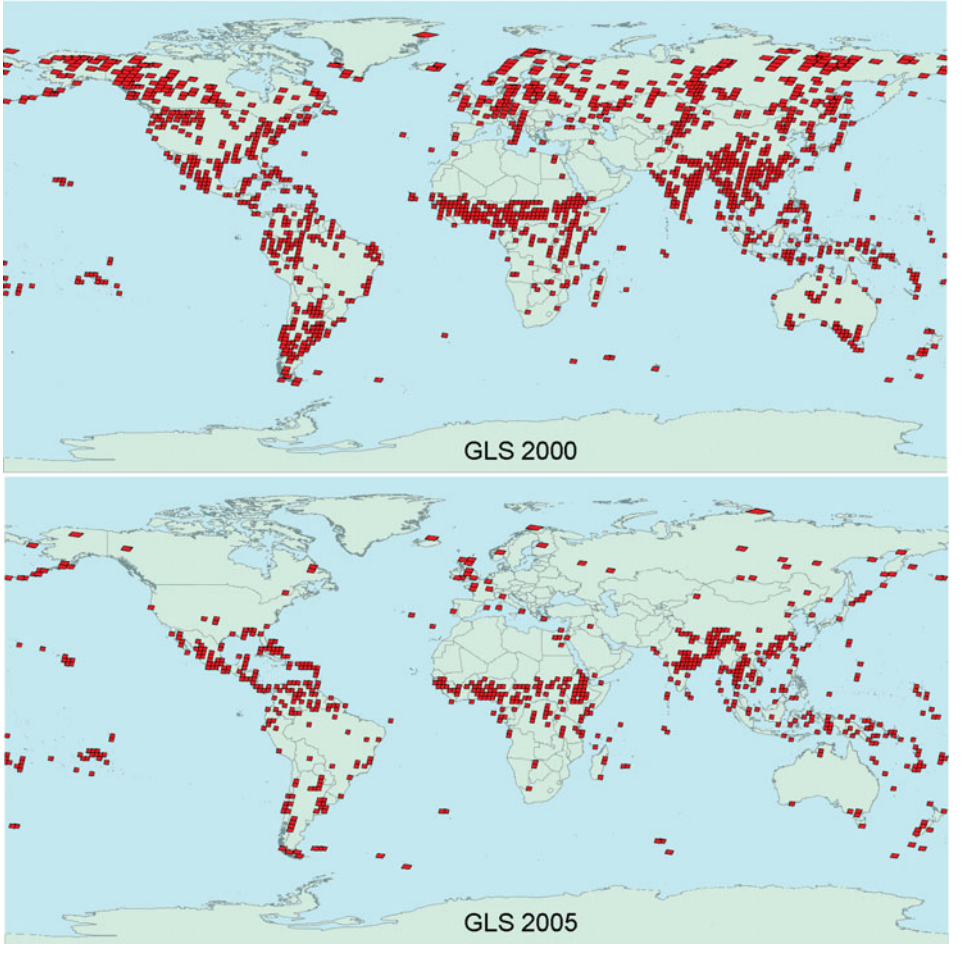

Figure 3. Substitutions (red quadrangles) made for GLS 2000 and 2005 because of phenological problems in the original GLS data-sets.

USGS is currently attempting to acquire Level 0 data and plans to reprocess them so that correct values can be derived and used.

Atmospheric correction of the Landsat images is based on the algorithm developed for the MODIS (Vermote *et al*. 2002) based on the 6S radiative transfer code. It was adopted for use with Landsat data and was implemented as part of the Landsat Ecosystem Disturbance Adaptive Processing System (LEDAPS) developed at NASA Goddard Space Flight Center (Masek *et al*. 2006, Huang *et al*. 2009a,b). As an adaptation of the MODIS Adaptive Processing System (Justice *et al*. 2002) for processing Landsat data, the LEDAPS allows rapid processing of large quantities of Landsat images to produce surface reflectance products from the raw radiometry. It has been used to produce a surface reflectance record consisting of over 2000 Landsat images over North America (Masek *et al*. 2006). Song *et al*. (2001) showed how use of surface reflectance can improve the change detection using Landsat data.

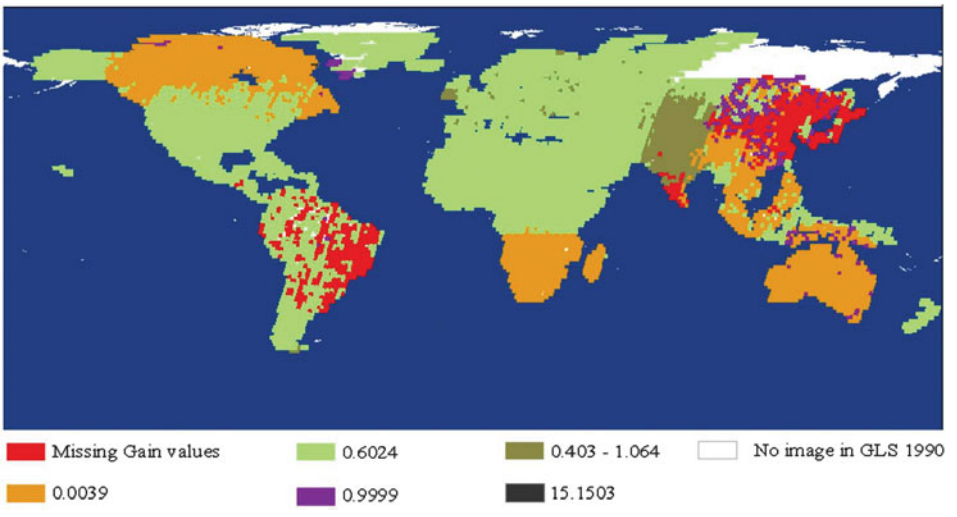

Figure 4. Scenes with problematic gain and bias values for GLS 1990. The color coding represents the different gain values for band 1. Other bands have different values, but the same spatial pattern.

The 6S radiative transfer code is used to compute the transmission, intrinsic reflectance, and spherical albedo for relevant atmospheric constituents (Vermote *et al.* 1997), and to calculate surface reflectance by compensating for atmospheric scattering and absorption effects on the TOA reflectance. The atmospheric constituents include ozone, water vapor, and aerosols. Ozone concentration was derived from the Total Ozone Mapping Spectrometer (TOMS) aboard the Nimbus-7, Meteor-3, and Earth Probe platforms as well as from NOAA's Television Infrared Observation Satellite Program's, Operational Vertical Sounder's, ozone data when TOMS data were not available. Column water vapor was taken from the reanalysis data of NOAA National Centers for Environmental Prediction (NCEP) (available at http://dss.ucar.edu/datasets/ds090.0/). Digital topography (1 km GTopo30) and NCEP seal level pressure data were used to adjust Rayleigh scattering to local conditions. Aerosol optical thickness was directly derived from the Landsat image using the dark, dense vegetation method of Kaufman *et al.* (1997).

Explicit atmospheric correction of MSS data is not currently possible because of the lack of shortwave infrared bands. Until recently it was also hindered by relatively poor knowledge of calibration coefficients but MSS calibration for Landsats 1–3 has recently been reworked and standardized (Markham and Helder in press), so it should be much improved. Instead, radiometric matching techniques can be used to adjust per-band radiometry to match a corresponding image. While this will not result in true surface reflectance, we believe it will be sufficient for many types of change detection over the long 15-year-period between the GLS 1975 and GLS 1990. Such techniques have been developed and used to normalize satellite data-sets in many land cover change studies (e.g. Hall *et al.* 1991, Elvidge *et al.* 1995, Cohen *et al.* 1998). An alternative is to explicitly correct for Rayleigh scattering and gaseous absorption of MSS using historical climatology data (e.g. NCEP) and just assume a constant aerosol loading.

Quality Assessment (QA) of every Landsat image is highly desirable because (1) errors could be introduced at any of the many steps between data acquisition and surface reflectance generation, and (2) QA results from one image are not usually extensible to another because each image is processed independent of other images. Because the MODIS on the Terra satellite and Landsat 7 are only half an hour apart following the same orbit, it has been possible to create an automated Landsat–MODIS Consistency Checking System that automatically matches Enhance Thematic Mapper Plus ETM + and MODIS observations and derives a set of agreement metrics (Gao *et al*. 2006, Feng *et al*. 2011). Since MODIS surface reflectance products have been assessed comprehensively (e.g. Vermote *et al*. 2002, Liang *et al*. 2002, Kotchenova and Vermote 2007, Vermote and Kotchenova 2008), and each of the six Landsat spectral bands overlaps with a MODIS band, they can be used to assess the quality of Landsat surface reflectance products. Our procedures involve the comprehensive checking of every single Landsat scene.

Most Landsat images have been found to have close agreement with MODIS reflectance products (Figure 5). The discrepancies between the Landsat and MODIS reflectance products are generally within the uncertainty allowed by instrument specifications – the greater of 0.5% absolute reflectance or 5% of the retrieved reflectance value. Where disagreements have been found, they are all explicable. The most common issues are cloud movement between Landsat and MODIS overpasses, saturation in a Thematic mapper (TM)/ETM + image but not MODIS, incorrect rescaling gains in Landsat metadata and corrupted Landsat images which needed to be replaced. In a few cases problematic MODIS data caused the disagreement: examples include the saturation of the MODIS 2.2 micron Short-wave Infrared (SWIR) band over very bright targets during the first few months after the Terra launch. Comparisons have also been made with Aeronet data and IKONOS reflectance data, and analysis of inter-annual stability of Landsat 5/7 reflectance time series. All indicate the satisfactory quality of the Landsat reflectance values (Feng *et al*. 2012).

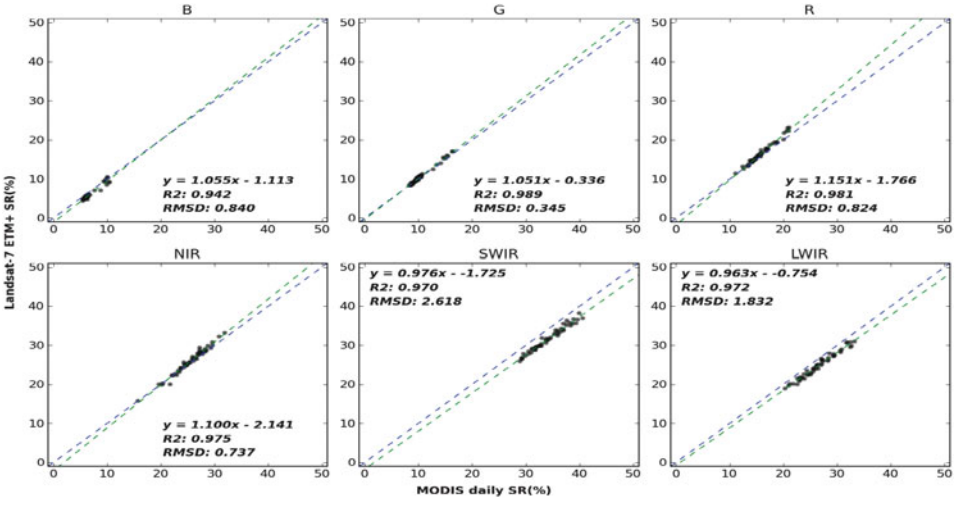

Figure 5. Typical agreement between ETM + and MODIS reflectance values for a single Landsat scene.

The orbit of Landsat 5 images is 8 days apart from that of Terra. Hence the viewing geometry of the images will be different and bidirectional effects will confuse the comparison. Hence it is recommended that the MODIS NBAR product is used where corrections for view angle effects have been made in assessing the Landsat surface reflectance values. While MODIS NBAR data can also be used to QA the Landsat 7 reflectance products, MODIS daily data provide a more direct comparison because Terra MODIS and Landsat images acquired on the same day are expected to have very similar values. Assuming temporal changes due to land cover change and inter-annual variability are relatively small within a Landsat scene, the MODIS NBAR may be used to QA pre-MODIS Landsat surface reflectance products. Correction of Landsat images for internal bidirectional effects especially in the tropics is desirable but has not yet been carried out by the authors for the global data-sets.

The Landsat Reflectance products are initially being made available through the Global Land Cover Facility (www.landcover.org).

Identifying pixels contaminated by cloud or cloud shadow is necessary to avoid them falsely flagging FCC or in providing incorrect retrievals of other land surface attributes (Huang *et al*. 2010). We have relied on the implementation of LEDAPS (Masek *et al*. 2006), which currently implements two cloud masks – a version of the Landsat Automated Cloud Cover Assessment algorithm (Irish 2000) and a more aggressive mask based on MODIS spectral tests (Ackerman *et al*. 1998). Shadows are calculated from the latter using the known solar geometry and an estimate of cloud height based on the temperature difference between known cloudy pixels and NCEP surface temperature. The two methods can be combined using a voting methodology in order to produce a cloud and cloud shadow mask.

5. Reducing the effects of terrain

The GLS data-sets have undergone orthorectification using procedures similar to those applied in the creation of the global GeoCover data-sets (Tucker *et al*. 2004). The National Imagery and Mapping Agency (now the National Geospatial Agency) provided geodetic control points to the Earth Satellite Corporation where they were used in data processing. The goal for the horizontal Root Mean Square Error (RMSE) of these data-sets is better than 50 m in positional accuracy. To match GLS 2000 as closely as possible, the GLS 2005 data-set is based on the same Digital Elevation Model (DEM) inputs as GLS 2000. Within the USA, the USGS National Elevation Data-set's digital topography was used, while Shuttle Radar Topography Mission (SRTM) data are used for the rest of the globe up to 60° in latitude. In far northern regions othorectification uses either the Canadian Digital Elevation Data (CDED) or Digital Terrain Elevation Data (DTED) topographic data-sets. Orthorectification significantly reduces the effort of georegistering images and makes the task of change detection much easier and more reliable. Nevertheless, the nominal RMSE values of 40–50 m are substantially greater than the pixel size and hence errors due to relatively small amounts of misregistration will inevitably occur (Townshend *et al*. 1992). The quality of the output scenes depends upon the accuracy of the geometric control and topography (Gutman *et al*. 2008). Some scenes may display geodetic errors greater than 50 m especially in mountainous areas and where the DEM was of poor quality.

Another issue relating to terrain is effects due to variations in illumination. Variations in the solar zenith and azimuth angles can lead to spurious differences in land cover being detected. Hence, especially in more rugged areas, it will be important to make terrain corrections. One such simple characterization is based on normalizing for the Illumination Condition factor (IL) which describes the incident solar radiation on any terrain slope facet:

$$\mathrm{IL} = \cos Z_{\bullet} \cos S + \sin Z_{\bullet} \sin S_{\bullet} \cos(\Phi_Z - \Phi_S)$$

where Z, the solar zenith angle; S, the slope angle; Φ_z, the solar azimuth angle; Φ_s, is the aspect angle of the incline surface.

The correction calculates the dependency of reflectance on IL within discrete ranges of vegetation greenness and then transforms the image radiometry to eliminate the dependency (Tan *et al.* 2010)

Figure 6 shows graphically the importance of such corrections in rugged areas where the calendar dates of the two images are different, though note in this case that the difference in date is quite modest. Without making topographic corrections spurious changes in land cover will frequently be identified. More sophisticated corrections could in principle be made allowing for diffuse radiation and reflection from surrounding terrain (e.g. Dubayah 1992).

6. Training data

Land cover characterization and change detection requires an effective classification algorithm which is in turn dependent on adequate training. To make global mapping at the Landsat resolutions feasible, automated methods requiring minimal human

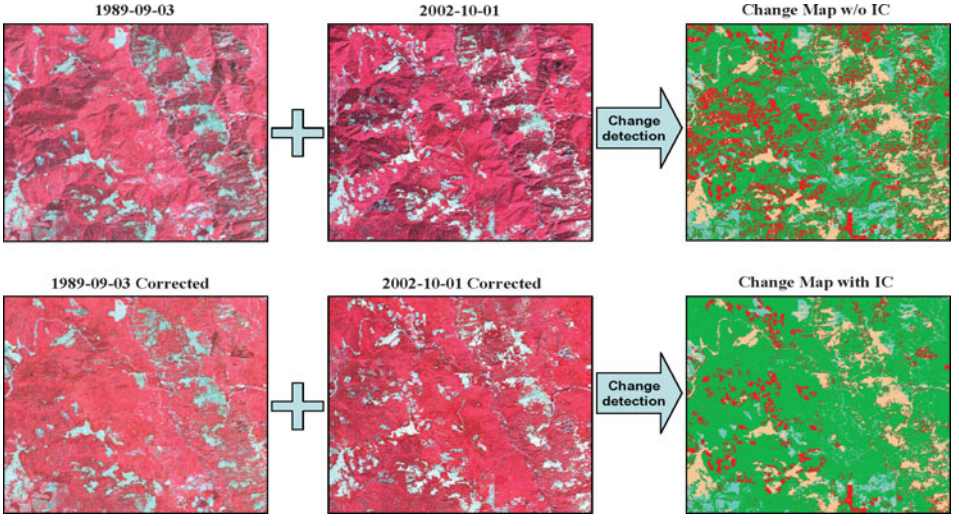

Figure 6. Illumination correction showing original sub-scenes (top row), the corrected images (bottom row) and the results of change detection without and with correction (right column). Many of the changes using the uncorrected images are clearly spurious. In the change maps (right column), persisting forest, persisting nonforest, forest loss and forest gain are in green, light pink, red and cyan, respectively.

inputs are critical. This section describes a training-data automation (TDA) procedure for deriving training data for forest change analysis. Their use in classification will be described in Section 7.

Gathering comprehensive training data for the whole of the Earth's land surface is clearly very challenging logistically, since collection of adequate training data is one of the most time-consuming components of land cover characterization and change detection using remote sensing. Although there are training data associated with several global land cover products at coarser resolutions of 250 m and coarser, their value for finer resolution Landsat data is less clear, nor are they usually made available in user-friendly forms for other users. For some countries such as the USA and Brazil considerable amounts of data are available, but the different definitions of land cover types throughout the world make such training data challenging to use without considerable care in cross comparisons.

For the task of mapping FCC globally, we have adopted a somewhat different approach. Note that we are concerned with cover type and we are not using the term 'forest' to indicate a type of land use. Specifically we first identify training data automatically (Huang *et al*. 2008). This procedure first uses local image windows to identify forest training samples (Figure 7). Automation is made possible by the following: (1) forests are one of the darkest vegetated surfaces in satellite images (Colwell 1974, Goward *et al*. 1994, Huemmrich and Goward 1997), (2) the presence

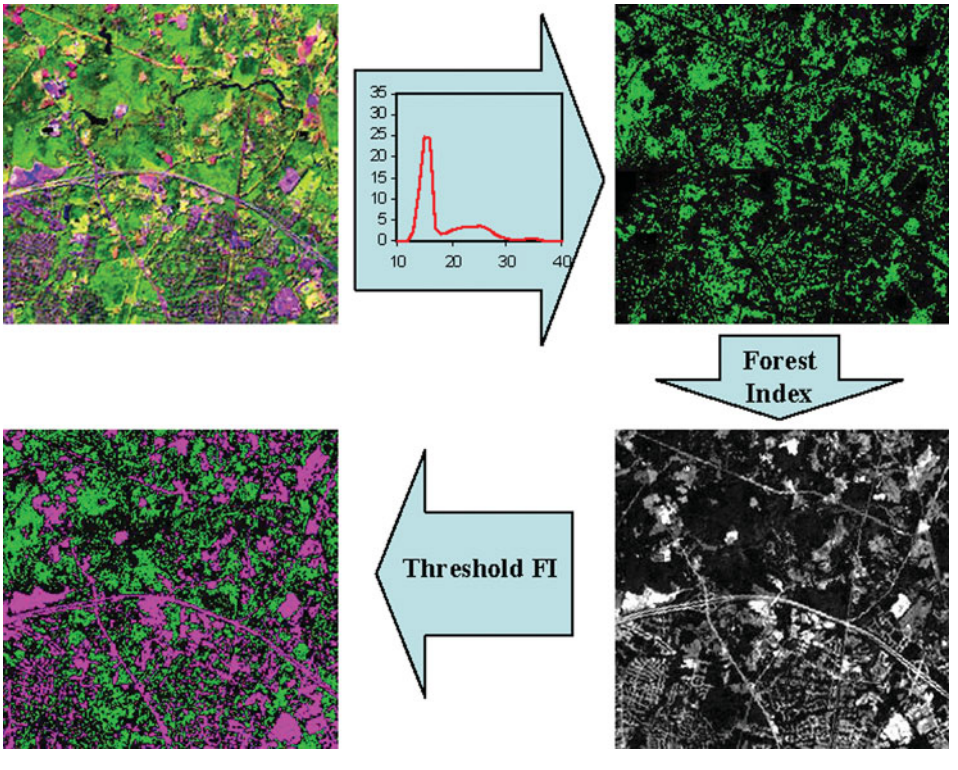

Figure 7. Training-data automation: an initial selection of training data is carried out by the use of the peak in the red response. Then a forest index is used to refine training areas for nonforest (Huang *et al*. 2008).

of forest within each local window is determined using to the MODIS vegetation continuous fields (VCF) tree cover product (Hansen *et al*. 2002).

The identified forest training pixels are then used to calculate a forest index (FI) measuring the likelihood of a pixel being forest in reality. The most unlikely forest pixels are identified as nonforest training pixels. Recognizing that the training pixels delineated in this way are mostly pure training samples, a neighborhood algorithm is used to locate training pixels close to class boundaries. Specifically, less pure forest pixels are chosen as forest training pixels if they immediately neighbor previously identified pure forest pixels. Similarly, less pure nonforest pixels are determined according to the FI value and nearness to nonforest training pixels. This method creates dense sets of global 'training data' adapted to local conditions, which are then used locally as input to the classifier, with each scene having its own unique training data-set.

An alternative but related approach is to use forest cover data directly from other sources. The MODIS VCF product at 250 m resolution can be used to identify similar sized training areas on Landsat scenes with an estimated percentage cover taken from the MODIS product. In this approach we derive training data with percentage cover associated with each and then estimate percentage forest cover and the amount of FCC using techniques such as regression trees.

These are two possibilities for automating the creation of global training data, but there will doubtless be many others. Both approaches will inevitably result in training data-sets with errors and hence there is the need to use information-extraction algorithms resistant to errors as described next.

7. Characterization of forest cover and change

The literature is replete with many different methods of land cover characterization. The authors' particular focus is in change detection and specifically in FCC detection. A wide range of techniques exist for cover change analysis using satellite data. Comprehensive reviews and comparisons of these techniques have been provided in several publications (e.g. Gordon 1980, Singh 1989, Lunetta and Elvidge 1998, Coppin *et al*. 2004, Lu *et al*. 2004). Many techniques have been tested with varying levels of success over small areas (e.g. Jha and Unni 1994, Cohen *et al*. 1998, Lyon *et al*. 1998, Tokola *et al*. 1999, Franklin *et al*. 2002). However, only a few were used to produce FCC products for large areas, and these typically required intensive human inputs in order to achieve satisfactory results (e.g. Skole and Tucker 1993, Townshend *et al*. 1995, Loveland *et al*. 2002, Huang *et al*. 2007).

As pointed out in the previous section producing globally consistent and reliable FCC products at affordable costs requires highly automated change detection algorithms requiring minimal human inputs. To meet this challenge we have developed a method integrating TDA and SVM.

Previously we have used decision tree algorithms to develop land cover classifications at global scales (e.g. Hansen *et al*. 1996, DeFries *et al*. 1998, Hansen *et al*. 2000). However, SVM has theoretical advantages and has demonstrated superior performance and hence provide a good solution for global FCC analysis. SVM is a group of relatively new machine learning algorithms designed to find optimal classification solutions (Vapnik 1998), which are achieved by using the optimal boundary between classes as the classification boundary. As shown in Figure 8,

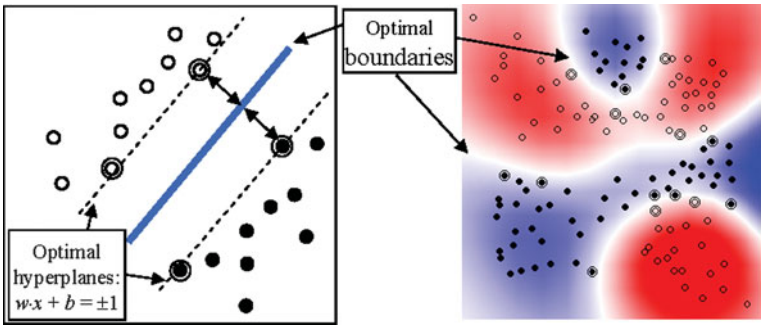

Figure 8. A hypothetical classification problem showing the optimal boundary defined by support vectors (circled points) and a pair of optimal hyperplanes for an arbitrary two-class problem with the classes represented by solid and empty points (left). Nonlinear optimal boundaries defined by SVM using the RBF kernel function (right) (Song 2010).

there can be many class boundaries that are sufficient to completely distinguish between classes for a given training data-set. SVM uses support vectors and a pair of optimal hyperplanes to define the optimal boundary. The optimal hyperplanes are defined using a vector w and are located by maximizing the distance between them.

The value of SVM compared with decision trees and neural networks has been demonstrated in several previous studies (e.g. Chan *et al.* 2001, Huang *et al.* 2002; Pal and Mather 2005). Subsequently we applied SVM for change detection and showed that the accuracies were close to those produced with intensive human interventions (Song *et al.* 2005).

A key feature of SVM is its resistance to error in training data, which is especially important because of our need to automate change detection given the very large size of the global data-sets. In experiments we progressively added noise representing error into training data and we have consistently found that SVM is more resistant to the introduction of random errors than other methods such as decision trees or neural networks (Figure 9)

Since training the SVM can be automated it is possible to automate the entire multi-temporal SVM classification approach for FCC analysis. Using the 1990 TM images and 2000 ETM + images, we tested the TDA–SVM method over 19 study areas selected from major forest biomes across the globe (Huang *et al.* 2008), with each test area being at least a complete Landsat scene. High-resolution IKONOS images and independently derived reliable reference data-sets were used to calculate accuracy estimates for the developed FCC products. Not only the overall accuracies of products were well above or near 90%, the class specific user's and producer's accuracies were also quite high, with over half of those values being over 90%, 30% being over 80%, and the remaining being over 70% (Table 2).

At the conclusion of the previous section we referred to an alternative procedure for deriving training data using the MODIS-derived VCF product. In this alternative procedure resultant training data are labeled with % forest cover using the MODIS product; this approach allows their use in estimating changes in the percentage cover rather than a discrete change from forest to nonforest.

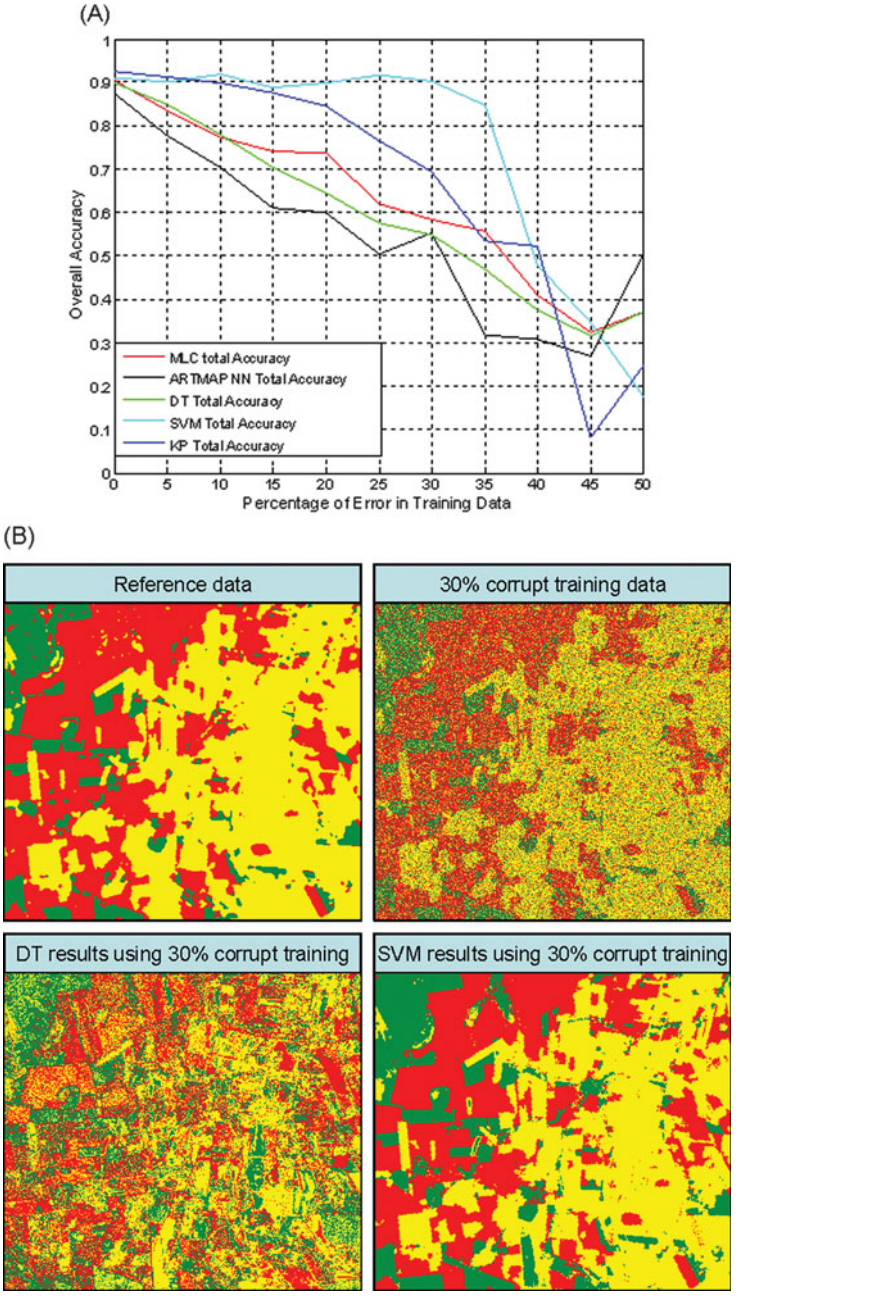

Figure 9. Impact of errors in training data on the performance of different classifiers. (A) Variation in classification accuracy for the maximum likelihood classifier (MLC), ARTMAP neural net (NN), decision tree (DT), support vector machines (SVM), and kernel perceptron (KP). (B) Graphical depiction of the impact of 30% training data error for DT and SVM. Persisting forest, persisting nonforest and forest loss are in green, yellow and red, respectively (Song 2010).

Table 2. Overall, user's and producer's accuracies (%) of TDA–SVM derived FCC products evaluated using independent reference data-set (N/A: accuracy was not calculated because the reference data did not have information for the concerned FCC class).

Accuracy measure	Persisting forest	Persisting nonforest	Forest loss	Forest gain
Eastern Virginia, USA, WRS2 path 15/row 34: overall accuracy = 92.7				
User's accuracy	96.7	94.9	88.2	74.5
Producer's accuracy	96.7	86.2	88.3	88.4
Southeastern Finland, WRS2 path 187/row 17: overall accuracy = 94.8				
User's accuracy	96.7	96.1	80.6	95.9
Producer's accuracy	97.9	93.3	96.3	82.2
Central Mississippi, USA, WRS2 path 22/row 37: overall accuracy = 89.4				
User's accuracy	95.8	92.2	85.7	72.6
Producer's accuracy	88.0	95.3	80.7	88.9
Central western Washington, USA, WRS2 path 46/row 27: overall accuracy = 94.4				
User's accuracy	93.4	93.0	98.2	100.0
Producer's accuracy	99.5	99.6	100.0	70.6
Connecticut, USA, WRS2 path 13/row 31: overall accuracy = 96.5				
User's accuracy	98.5	95.2	88.2	80.5
Producer's accuracy	99.7	92.2	100.0	77.6
Eastern Paraguay, WRS2 path 224/row 78: overall accuracy = 94.2				
User's accuracy	76.5	95.9	83.9	N/A
Producer's accuracy	93.0	91.3	80.4	N/A
Western Paraguay, WRS2 path 228/row 75: overall accuracy = 89.6				
User's accuracy	89.8	96.4	85.1	N/A
Producer's accuracy	93.1	79.7	91.8	N/A

8. Post-processing

Post-processing is frequently carried out to reduce errors in the resultant products. In the past this has often been carried out using human interpreters who manually modify images (e.g. Huang *et al*. 2007). For a global data-set such human intervention is impractical if applied to the whole globe. We have implemented a consistency and quality checking (CQC) process, which uses other data sources to identify areas with major discrepancies from existing sources. This process is designed to highlight scenes where the FCC products' performance may be unsatisfactory.

In the CQC process, the FCC products are used to calculate percent forest cover (PFC) within 10-km grid cells, which are then be compared with values from the MODIS VCF product. A good FCC product for a particular WRS2 tile should have PFC values consistent with those derived using an existing reliable land cover product (Figure 10). Inconsistencies between the two sets of PFC values are indicators of uncertainties in either the FCC product or the existing land cover product, or both. When a FCC product is found problematic through the CQC process, additional training data are introduced and the images are reclassified using the SVM to improve the FCC product. The additional training data will be derived by extracting from our global training data pools we have accumulated through

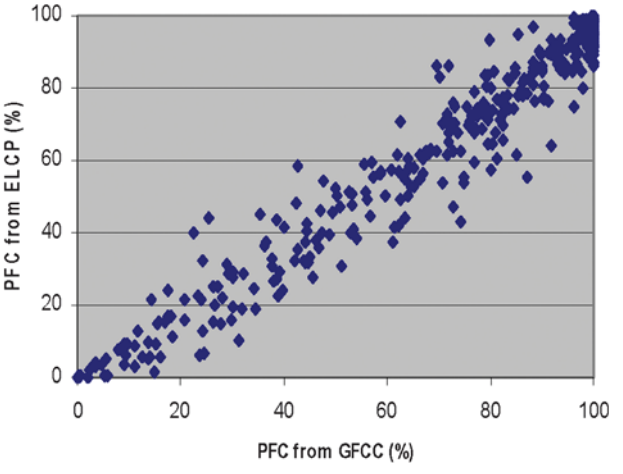

Figure 10. Percent forest cover (PFC) within 10-km grid cells for the 2000 epoch calculated using a TDA–SVM derived FCC product and the standard MODIS VCF tree cover product. The near 1:1 relationship between the two sets of PCF values is an indicator of the high quality of the TDA–SVM derived FCC product.

previous land cover activities (DeFries and Townshend 1994, DeFries *et al*. 1995, 1998, Hansen *et al*. 2000, 2002) and using ultra-fine high-resolution images from systems such as IKONOS, QuickBird, and OrbView.

Doubtless there are alternatives to these proposed approaches but any must include a very high degree of automation because of the enormous number of scenes to process globally.

9. Estimation of product error

Estimation of errors in the resultant products is essential but poses particular challenges, because of the variability in appearance of land cover types across the globe and the absence of reliable test data-sets. High-resolution images with 5 m or less resolution can be a valuable source of information because for some cover types at least they are readily recognizable by visual interpretation. Forest cover and water bodies fall into this category. Figure 11 shows a web-based tool allowing rapid labeling of FCC on multi-temporal Landsat images using coregistered very fine resolution satellite data.

Comparing products with others that have had their accuracy assessed is an alternative approach as previously shown in Figure 10. We can extend this approach by comparing the results with a synthesis of multiple products. Song *et al*. (2011) used a regression tree model to integrate forest cover from GLC 2000, MODIS VCF, GLCC, GlobCover, and the standard MODIS classification to create a 5-km product. Comparison with validated North American products indicates that this synthesis is substantially more accurate than any of the individual products. The synthesis can now be used elsewhere in the world to assess the reliability of our forest products. An alternative approach would be to use crowd-sourcing derived data as in the Geo-Wiki Project (Fritz *et al*. 2009). Considerable effort will be needed to apply

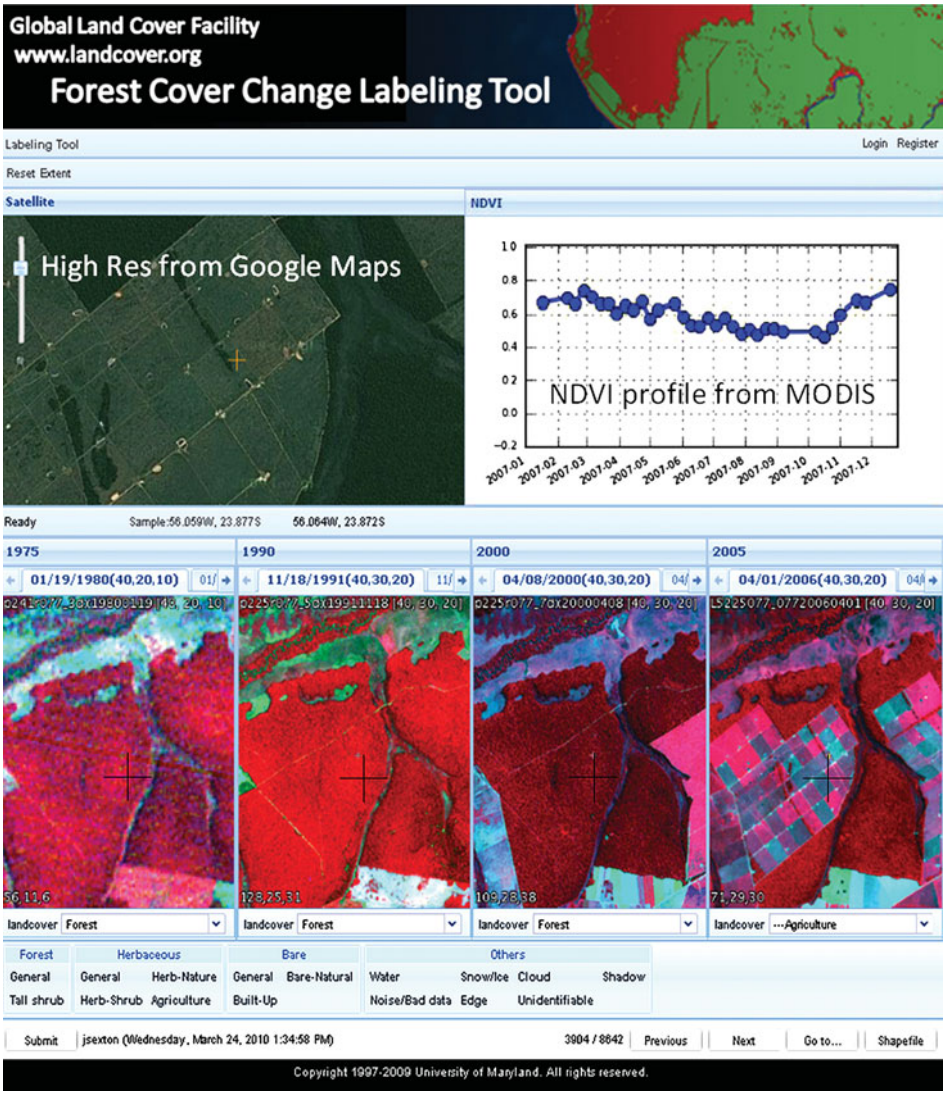

Figure 11. Web-based forest change labeling tool allowing rapid labeling of forest cover and change using fine-resolution imagery automatically coregistered to multi-temporal Landsat images.

these methods comprehensively and create statistically robust error estimates globally and locally.

10. Concluding comments and future implications

The assembly of global Landsat data collections such as those of the GLS coupled with rapidly declining cost of computing and improved analytical methods makes feasible the monitoring of the whole Earth's land surface using Landsat data.

Nevertheless, there are major challenges in the creation of internally consistent products with known statistical errors. For example many images in the GLS compilations are sub-optimal for forest cover discrimination because they are leaf-off. We have shown that it is often possible to obtain substitute images to replace them. Some gaps in the original GLS data-sets especially GLS 1975 have also been filled. Corrections for topography are also needed in many areas.

Use of the data-sets is made much easier by the production of Landsat surface reflectance images. We have demonstrated how these can be created using methods based on MODIS algorithms. MODIS data can also be used to evaluate the performance of the Landsat surface reflectance images. With some explicable and identified exceptions the Landsat images provide a very good representation of surface reflectance. The incorrect calibration coefficients provided for many scenes in GLS 1990 have prevented the creation of reflectance images, but it will be possible to replace them with correct values.

Land cover characterization is hindered by the paucity of consistent high-quality training data. For forest cover the approach we adopted to overcome this issue is automatically to identify 'training data' and then apply classification methods which are robust to errors in the training data. We have described methods for identifying potentially poorly characterized images by use of independently created products. In this way the number of images requiring more intensive post-processing is considerably reduced. Estimation of errors in the resultant products is hindered by the absence of globally representative reliable test data-sets. Some approaches to reduce this problem have been proposed in this article. These have to be of very high quality, otherwise estimated errors may conflate errors in the product and the test data-sets themselves.

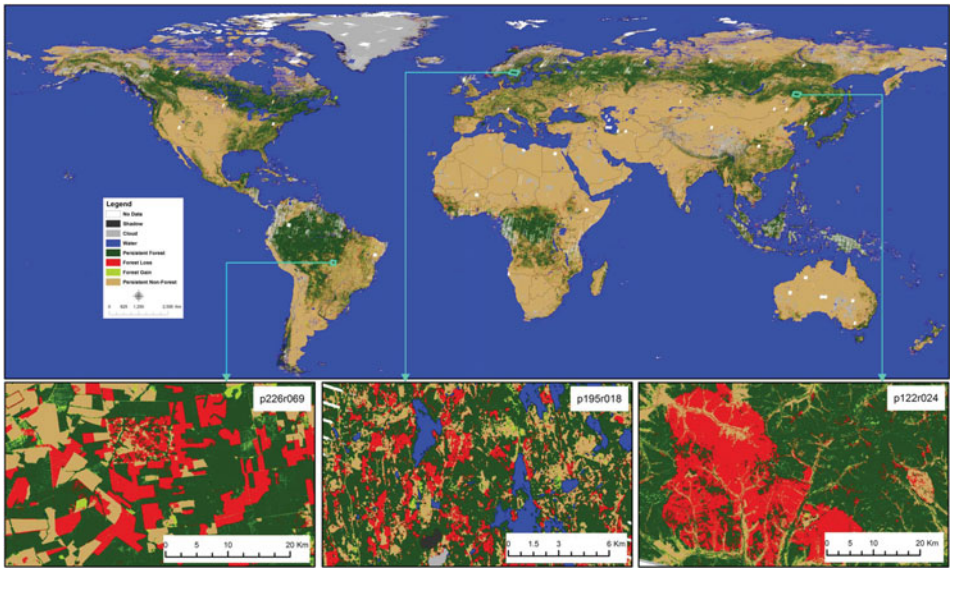

Figure 12. Preliminary global forest cover change (FCC) map derived using the GLS 2000 and 2005 datasets. The three full resolution examples (each approximately 25 km across) show deforestation in Lucas do Rio Verde, Brazil (lower left), logging and harvest in south central Sweden (lower center), FCC primarily due to burning in northeastern China (lower right).

Using the methods described in this paper (Figure 12), we present a working prototype global product of forest cover and change defined as those areas with greater than 30% cover. Currently extensive estimation of errors is being carried out and once completed a digital version will be made available through the Global Land Cover Facility. Although reliable estimates of errors for this product remain to be calculated results of comparisons with products that have had error estimation (see Figure 10) encourage us to believe that our approach has significant merit. We believe this is the first global product of any land cover type at Landsat resolution, specifically for forest cover and FCC to be reported in the refereed literature.

A fundamental problem with any approach using the GLS data-sets is that each contains only a single image, whereas it is well established that multi-temporal images are of considerable value for characterizing cover types because of their different phenologies. It is of course possible in principle to access the archive of Landsat data at USGS–EDC (EROS Data Center) for free to acquire additional images, but the task of selecting even one additional image for each scene would be considerable. Nevertheless, improvements in performance will likely require at least two images for each scene so that simple indicators of vegetation phenology can be used.

Can our automated approach for training identification be applied to other types of land cover? There is reasonable expectation that will be possible for some categories; for example, water has a sufficiently distinctive spectral response that such an approach is likely to be successful. In the creation of a 250-m global land–water mask, for all those areas north of the coverage of SRTM at 55°N, Landsat data were used successfully to identify water bodies (Carroll *et al.* 2009) and that change detection is feasible.

Changes in data policy were crucial in allowing the creation of global Landsat collections. Without the policy of making Landsat images freely available the GLS would have been prohibitively expensive for most users. In creating global sets of medium resolution images there is in principle no reason to rely solely on Landsat images, but data policies restrict their availability. Note that for GLS 2005 some data from ASTER have been used. However, use of other sources is often restricted by charging and copyright restrictions. Government policies may often limit use of data in quite complex ways. Considering only Chinese data, some data are openly available, whereas others are restricted in use. China–Brazil Earth Resources Satellites (CBERS) archives are now openly available to all (as are those in Brazil for CBERS), but open availability of data from the more recent Huan Jing (HJ) satellites is openly available only to Chinese users though with some restricted availability for others. Beijing-1 satellite is now operated on a commercial basis. A liberalization of data policies in China and elsewhere would do much to improve the quality of global medium resolution data-sets: for example there would be a considerable potential for GLS 2010 to be improved by replacing images with deficiencies such as poor matching phenology and high cloud cover and in selecting images closer the nominal 2010 date.

One of the constraints in creating global products is dealing with all the separate individual scenes. The Web-Enabled Landsat Data (WELD) approach of Roy *et al.* (2010) in creating seamless mosaics for the continental US potentially has much to offer users if the approach was applied globally. Moreover, its selection of 'optimal' pixels from multiple images can do much to reduce the effects of clouds and other image artifacts.

In conclusion the prospect of global products derived from Landsat data at last allows the realization of the full potential of Landsat for global land cover characterization and monitoring. But successful use of existing global compilations requires considerable understanding of their characteristics and limitations as we have shown. Creating reliable global products at Landsat resolutions poses major challenges but the possibilities of overcoming them and the potential resultant opportunities have been demonstrated in this article.

Acknowledgements

The research dealt here was supported by the following awards from NASA: MEASURES: NNX08AP33A and LCLUC: NNX08AN72G. We also gratefully acknowledge the earlier support from the NASA Terrestrial Ecology Program which led to the creation of LEDAPS on which much of this work is based. We acknowledge the help of two people in particular from USGS EROS: Gyanesh Chander helped to identify the GLS 1990 images that have most recent USGS calibration coefficients ($\sim$50% of the GLS 1990 data-set). Rachel Headley helped us obtain the GLS data-sets. She also helped significantly with our reordering of the GLS 1990 images that had good calibration coefficients. We are also grateful to Yosio Shimabukuro and Egidio Arai of the Brazilian National Institute for Space Research (INPE) for help in acquiring the MSS images needed to fill the large data gap over northern South America in the GLS 1975 data-set.

References

Ackerman, S.A. *et al*., 1998. Discriminating clear sky from clouds with MODIS. *Journal of Geophysical Research D: Atmospheres*, 103 (D24), 32,141–32,157.

Arvidson, T., Gasch, J., and Goward, S.N., 2001. Landsat-7's Long Term Acquisition Plan – an innovative approach to building a global imagery archive. *Remote Sensing of Environment*, 78, 13–26.

Band, L.E., 1993. Effect of land surface representation on forest water and carbon budgets. *Journal of Hydrology*, 150, 749–772.

Carroll, M.L, *et al*., 2009. A new global raster water mask at 250 meter resolution. *International Journal of Digital Earth*, 2 (4), 291–308.

Chan, J.C., Huang, C., and DeFries, R., 2001. Enhanced algorithm performance for land cover classification from remotely sensed data using bagging and boosting. *IEEE Transactions on Geoscience and Remote Sensing*, 39 (3), 693–695.

Chander, G., *et al*., 2004. Landsat-5 TM reflective-band absolute radiometric calibration. *IEEE Transactions on Geoscience and Remote Sensing*, 42, 2747–2760.

Chander, G., Markham, B.L., and Helder, D.L., 2009. Summary of current radiometric calibration coefficients for Landsat MSS, TM, ETM+, and EO-1 ALI sensors. *Remote Sensing of Environment*, 113, 893–903.

Cohen, W.B., *et al*., 1998. An efficient and accurate method for mapping forest clearcuts in the Pacific Northwest using Landsat imagery. *Photogrammetric Engineering & Remote Sensing*, 64, 293–300.

Colwell, J.E., 1974. Vegetation canopy reflectance. *Remote Sensing of Environment*, 3, 174–183.

Coppin, P., *et al*., 2004. Digital change detection methods in ecosystem monitoring: a review. *International Journal of Remote Sensing*, 25, 1565–1596.

DeFries, R., Hansen, M., and Townshend, J.R.G., 1995. Global discrimination of land cover types from metrics derived from AVHRR Pathfinder data. *Remote Sensing of Environment*, 54, 209–222.

DeFries, R.S. and Townshend, J.R.G., 1994. NDVI-derived land cover classifications at a global scale. *International Journal of Remote Sensing*, 15, 3567–3586.

DeFries, R.S., *et al*., 1998. Global land cover classifications at 8km spatial resolution: the use of training data derived from Landsat imagery in decision tree classifiers. *International Journal of Remote Sensing*, 19, 3141–3168.

DeFries, R., *et al*., 2002. Carbon emissions from tropical land use change based on satellite observations for the 1980s and 90s. *Proceeding National Academy of Sciences USA*, 99, 14256–14261.

Dubayah, R., 1992. Estimating net solar radiation using Landsat Thematic Mapper and digital elevation data. *Water Resources Research*, 28 (9), 2469–2484.

Elvidge, C.C., *et al*., 1995. Relative radiometric normalization of Landsat multispectral scanner (MSS) data using an automatic scattergram-controlled regression. *Photogrammetric Engineering & Remote Sensing*, 61, 1255–1260.

FAO, 2001. *Global forest resources assessment 2000 – Main Report*. Rome: FAO, FAO Forestry Paper No. 140.

Feng, M., *et al*., 2011. Quality assessment of Landsat surface reflectance products using MODIS data. *Computers and Geosciences*, 36, 9–22.

Feng, M., *et al*., 2012. Global, long-term surface reflectance records from Landsat. *Remote Sensing of Environment* (submitted).

Franklin, S.E., *et al*., 2002. Change detection and landscape structure mapping using remote sensing. *Forestry Chronicle*, 78, 618–625.

Franks, S. and Headley, R.M.K. 2008. Large area scene selection interface (LASSI) methodology of selecting Landsat imagery for the global land survey 2005. *Proceedings Pecora 17 the Future of Land Imaging Going Operational*, 18–20 November 2008, Colorado: Denver.

Fritz, S., *et al*., 2009. Geo-Wiki.Org: the use of crowdsourcing to improve global land cover. *Remote Sensing*, 1 (3), 345–354.

Gao, F., *et al*., 2006. On the blending of the Landsat and MODIS surface reflectance: predicting daily Landsat surface reflectance. *IEEE Transactions on Geoscience and Remote Sensing*, 44, 2207–2218.

GCOS, 2004. *Implementation plan for the global observing system for climate in support of the UNFCCC*. Geneva: Global Climate Observing System, GCOS – 92 (WMO/TD No. 1219).

Gordon, S., 1980. Utilizing Landsat imagery to monitor land use change: a case study of Ohio. *Remote Sensing of Environment*, 9, 189–196.

Goward, S.N., Huemmrich, K.F., and Waring, R.H., 1994. Visible-near infrared spectral reflectance of landscape components in western Oregon. *Remote Sensing of Environment*, 47, 190–203.

Gutman, G., *et al*., 2008. Towards monitoring land-cover and land-use changes at a global scale: the global land survey 2005. *Photogrammetric Engineering & Remote Sensing*, 74 (1), 6–10.

Hall, F.G., *et al*., 1991. Radiometric rectification: toward a common radiometric response among multidate, multisensor images. *Remote Sensing of Environment*, 35, 11–27.

Hansen, M., Dubayah, R., and DeFries, R., 1996. Classification trees: an alternative to traditional land cover classifiers. *International Journal of Remote Sensing*, 17, 1075–1081.

Hansen, M., *et al*., 2000. Global land cover classification at 1 km spatial resolution using a classification tree approach. *International Journal of Remote Sensing*, 21, 1331–1364.

Hansen, M.C., *et al*., 2002. Towards an operational MODIS continuous field of percent tree cover algorithm: examples using AVHRR and MODIS data. *Remote Sensing of Environment*, 83, 303–319.

Hansen, M., *et al*., 2008. Humid tropical forest clearing from 2000 to 2005 quantified using multi-temporal and multi-resolution remotely sensed data. *Proceedings National Academy of Sciences USA*, 105 (27), 9439–9444.

Hansen, M.C., *et al*., 2010. Quantification of global gross forest cover loss. *Proceedings National Academy of Sciences USA*, 107, 8650–8655.

Houghton, R.A., 1998. Historic role of forests in the global carbon cycle. *In*: G.H. Kohlmaier, M. Weber, and R.A. Houghton, eds. *Carbon dioxide mitigation in forestry and wood industry.* Berlin: Springer, 1–24.

Huang, C., Davis, L.S., and Townshend, J.R.G., 2002. An assessment of support vector machines for land cover classification. *International Journal of Remote Sensing*, 23, 725–749.

Huang, C., *et al*., 2007. Rapid loss of Paraguay's Atlantic forest and the status of protected areas – a Landsat assessment. *Remote Sensing of Environment*, 106, 460–466.

Huang, C., *et al*., 2008. Use of a dark object concept and support vector machines to automate forest cover change analysis. *Remote Sensing of Environment*, 112, 970–985.
Huang, C., *et al*., 2009a. Development of time series stacks of Landsat images for reconstructing forest disturbance history. *International Journal of Digital Earth*, 2, 195–218.
Huang, C., *et al*., 2009b. Dynamics of national forests assessed using the Landsat record: case studies in eastern U.S. *Remote Sensing of Environment*, 113, 1430–1442.
Huang, C., *et al*., 2010. Automated masking of cloud and cloud shadow for forest change analysis. *International Journal of Remote Sensing*, 31, 5449–5464.
Huemmrich, K.F. and Goward, S.N., 1997. Vegetation canopy PAR absorptance and NDVI: an assessment for ten tree species with the SAIL model. *Remote Sensing of Environment*, 61, 254–269.
Irish, R., 2000. Landsat 7 automatic cloud cover assessment (ACCA). *In*: S.S. Shen and M.R. Descour, eds. *Algorithms for multispectral, hyperspectral, and ultraspectral imagery IV,* Vol. 4049. Orlando: SPIE, 348–355.
Jha, C.S. and Unni, N.V.M., 1994. Digital change detection of forest conversion of a dry tropical Indian forest region. *International Journal of Remote Sensing*, 15, 2543–2552.
Justice, C.O., *et al*., 2002. An overview of MODIS Land data processing and product status. *Remote Sensing of Environment*, 83, 3.
Kaufman, Y.D., *et al*., 1997. Passive remote sensing of tropospheric aerosol and atmospheric correction for the aerosol effect. *Journal of Geophysical Research*, 102 (D14), 16815–16830.
Kim, D.H., *et al*., 2011. Methodology to select phenologically suitable Landsat scenes for forest change detection. *Proceedings Geoscience and Remote Sensing Symposium (IGARSS)*, 24–29 July 2011. Vancouver: IEEE International, 2613–2616. doi: 10.1109/IGARSS.2011.6049738
Kotchenova, S.Y. and Vermote, E.F., 2007. Validation of a vector version of the 6S radiative transfer code for atmospheric correction of satellite data. Part II. Homogeneous Lambertian and anisotropic surfaces. *Applied Optics*, 46 (20), 4455–4464.
Lal, R., 1995. *Sustainable management of soil resources in the humid tropics*. New York: United Nations University Press, 146.
Liang, S., *et al*., 2002. Validating MODIS land surface reflectance and albedo products: methods and preliminary results. *Remote Sensing of Environment*, 83, 149–162.
Loveland, T.R., *et al*., 2002. A strategy for estimating the rates of recent United States land-cover changes. *Photogrammetric Engineering & Remote Sensing*, 68, 1091–1099.
Lu, D., *et al*., 2004. Change detection techniques. *International Journal of Remote Sensing*, 25, 2365–2407.
Lunetta, R.S. and Elvidge, C.D., 1998. *Remote sensing change detection: environmental monitoring methods and applications*. Chelsea, MI: Ann Arbor Press, 318.
Lyon, J.G., *et al*., 1998. A change detection experiment using vegetation indices. *Photogrammetric Engineering & Remote Sensing*, 64, 143–150.
Markham, B.L. and Helder, D.L. in press. Forty-year calibrated record of earth-reflected radiance from Landsat: a review. *Remote Sensing of Environment*.
Masek, J.G., *et al*., 2006. A Landsat surface reflectance dataset for North America, 1990–2000. *IEEE Geoscience and Remote Sensing Letters*, 3, 68–72.
Pal, M. and Mather, P.M., 2005. Support vector machines for classification in remote sensing. *International Journal of Remote Sensing*, 26, 1007–1011.
Pandey, D.N., 2002. Sustainability science for tropical forests. *Conservation Ecology*, 6, 13.
Roy, D.P., *et al*., 2010. Web-enabled Landsat Data (WELD): Landsat ETM + composited mosaics of the conterminous United States. *Remote Sensing of Environment*, 114, 35–49.
Singh, A., 1989. Digital change detection techniques using remotely-sensed data. *International Journal of Remote Sensing*, 10, 989–1003.
Skole, D.L., Salas, W.A., and Taylor, V. 1998. *Global observation of forest cover: fine resolution data and product design strategy report of a workshop*. Paris: CNES, GOFC Report No. 3, 29.
Skole, D. and Tucker, C., 1993. Tropical deforestation and habitat fragmentation in the Amazon: satellite data from 1978 to 1988. *Science*, 260, 1905–1910.
Song, C., *et al*., 2001. Classification and change detection using Landsat TM data: when and how to correct atmospheric effects? *Remote Sensing of Environment*, 75, 230–244.

Song, K. 2010. *Tackling uncertainties and errors in the satellite monitoring of forest cover change*. Unpublished thesis (PhD). University of Maryland, College Park.
Song, K., *et al*., 2005. Improving automated detection of land cover change for large areas using Landsat data. *Third international workshop on the analysis of multi-temporal remote sensing images,* Biloxi, MS: CD ROM.
Song, X.P., *et al*., 2011. An assessment of global forest cover maps using regional higher-resolution reference data sets. *Proceedings Geoscience and Remote Sensing Symposium, (IGARSS) Symposium*, 24–29 July 2011, Vancouver: IEEE International, 752–755.
Steininger, M.K., *et al*., 2001. Tropical deforestation in the Bolivian Amazon. *Environmental Conservation*, 28, 127–134.
Tan, B., *et al*., 2010. An illumination correction algorithm on Landsat-TM data. *Geoscience and Remote Sensing Symposium (IGARSS) 2010 IEEE Proceedings*, 25–30 July 2010, Honolulu, Hawaii: IEEE International, 1964–1967.
Tokola, T., Lofman, S., and Erkkila, A., 1999. Relative calibration of multitemporal Landsat data for forest cover change detection. *Remote Sensing of Environment*, 68, 1–11.
Townshend, J.R.G. and Justice, C.O., 1988. Selecting the spatial resolution of satellite sensors required for global monitoring of land transformations. *International Journal of Remote Sensing*, 9, 187–236.
Townshend, J.R.G., *et al*., 1992. The effect of misregistration on the detection of vegetation change. *IEEE Transactions on Electronic Engineers Geosciences and Remote Sensing*, 30 (5), 1054–1060.
Townshend, J.R.G., *et al*., 1995. The NASA Landsat pathfinder humid tropical deforestation project. *Land satellite information in the next decade. ASPRS conference*, 25–28 September 1995, Vienna: American Society for Photogrammetry and Remote Sensing, VI, IV–76 to IV–87.
Townshend, J.R., *et al*., 2004. Meeting the goals of GOFC. *In*: G. Gutman, *et al*., eds. *Land change science*. Dordrecht: Kluwer Academic Publishers, 31–51.
Townshend, J.R., *et al*., 2010. International coordination of satellite land observations: integrated observations of the land. *In*: B. Ramchandran, C.O. Justice, and M.J. Abrams, eds. *Land remote sensing and global environmental change: NASA's earth observing system and the science of ASTER and MODIS*. New York: Springer-Verlag, 835–56.
Tucker, C.J. and Townshend, J.R.G., 2000. Strategies for tropical forest deforestation assessment using satellite data. *International Journal of Remote Sensing*, 21, 1461–1472.
Tucker, C.J., Grant, D.M., and Dykstra, J.D., 2004. NASA's global orthorectified Landsat data set. *Photogrammetric Engineering & Remote Sensing*, 70, 313–322.
USGCRP, 1999. *A U.S. carbon cycle science plan*. Washington, DC: U.S. Global Change Research Program.
Vapnik, V.N., 1998. *Statistical learning theory: adaptive and learning systems for signal processing, communications, and control*. New York: John Wiley & Sons, Inc., 736.
Vermote, E.F., El Saleous, N.Z., and Justice, C.O., 2002. Atmospheric correction of MODIS data in the visible to middle infrared: first results. *Remote Sensing of Environment*, 83, 97–111.
Vermote, E.F. and Kotchenova, S., 2008. Atmospheric correction for the monitoring of land surfaces. *Journal of Geophysical Research-Atmospheres*, 113 (D23), D23S90.
Vermote, E.F., *et al*., 1997. Atmospheric correction of visible to middle-infrared EOS-MODIS data over land surfaces: background, operational algorithm and validation. *Journal of Geophysical Research*, 102 (D14), 17131–17141.
Zhang, Q., *et al*., 2005. Mapping tropical deforestation in Central Africa. *Environmental Monitoring and Assessment*, 101 (1–3), 69–83.

Appendix 1 Contributions of co-authors

John R. Townshend: PI
Jeffrey G. Masek: Co-PI, Surface reflectance implementation and change detection.
Chengquan Huang: Change detection algorithm and GLS data assessment.
Eric. F. Vermote: Surface reflectance algorithms.
Feng Gao: Implementation and refinement of surface reflectance.

Saurabh Channan: Project Manager, system development, data processing and distribution.
Joseph Sexton: Surface reflectance assessment, and change algorithm enhancement.
Min Feng Surface reflectance assessment, implementation of change detection algorithms.
Raghuram Narasimhan: Data analyst and system architect.
Dohyung Kim: Phenology improvements.
Kuan Song: Support vector procedures.
Danxia. Song: Data analyst.
Xiao-Peng Song: Post-processing enhancement for agriculture and semi-arid areas.
Praveen Noojipady: Algorithm refinement.
Bin Tan: Terrain illumination correction.
Matthew C. Hansen: Vegetation Continuous Fields product.
Mengxue Li: Data policy.
Robert E. Wolfe: Implementation of MODIS products.